

**SIMULATION OF OPEN CHANNEL TURBULENT FLOW OVER BRIDGE
 DECKS AND FORMATION OF SCOUR HOLE BENEATH THE BRIDGE
 UNDER FLOODING CONDITIONS**

**Bishwadipa Adhikary, Pradip Majumdar,
 and Milivoje Kostic**
 Department of Mechanical Engineering
 Northern Illinois University
 DeKalb, IL U.S.A.

Steven A. Lottes
 Argonne National Laboratory
 West Chicago, IL U.S.A.

ABSTRACT

This study is focused on the simulation of open channel turbulent flow over flooded laboratory scale bridge decks and formation of scour holes under various flooding conditions. Solutions for turbulent flow field are based on Reynolds Averaged Navier-Stokes (RANS) equations and turbulence closure models using the STAR-CD commercial computational fluid dynamics (CFD) software. An iterative computational methodology is developed for predicting equilibrium scour profiles using the single-phase flow model with a moving boundary formulation. The methodology relies on an empirical correlation for critical bed shear stress that is used to characterize the condition for onset of sediment motion and an effective bed roughness that is a function of sediment particle size. The computational model and iterative methodology were stable and converged to an equilibrium scour hole shape and size that compares reasonably well with experiment using a constant critical shear stress value.

1. NOMENCLATURE

| Symbol | Unit | Description |
|----------|-------|--------------------------------------|
| A_F | m^2 | Frontal area |
| A_P | m^2 | Planar area normal to gravity vector |
| C_D | - | Coefficient of drag |
| C_L | - | Coefficient of lift |
| d | mm | Sediment diameter |
| d_{50} | mm | Median sediment diameter |
| d_* | - | Dimensionless sediment diameter |
| F_D | N | Drag force |
| F_L | N | Lift force |

| | | |
|--------------|-----------|--|
| Fr | - | Froude number |
| g | m/s^2 | Acceleration due to gravity |
| h_b | m | Height of bridge above bed |
| h_u | m | Height of the water free surface above channel bed |
| h^* | - | Inundation ratio |
| k | m^2/s^2 | Turbulence kinetic energy |
| L_{bridge} | m | Length of the bridge |
| L_c | m | Characteristic length |
| M | - | Coefficient of uniformity |
| S | - | Specific gravity of the bed sediment |
| s | m | Bridge deck height |
| V_u | m/s | Upstream velocity |
| W | m | Width of the bridge |
| W_s | m/s | Settling velocity |
| X | m | Coordinate in primary flow direction |
| Y | m | Coordinate normal to flume bed |
| y | cm | Scour depth at a specific x location |

Greek Symbols

| | | |
|---------------|-----------|------------------------------------|
| ν | m^2/s | Kinematic viscosity of water |
| ρ | kg/m^3 | Density of water |
| ε | m^2/s^3 | Turbulence dissipation rate |
| ω | $1/s$ | Specific dissipation rate |
| τ_c | N/m^2 | Critical shear stress |
| ρ_s | kg/m^3 | Density of sediment |
| τ_x | N/m^2 | Bed shear stress along X direction |

2. INTRODUCTION

The design of new bridges and scour risk evaluation of existing bridges can benefit greatly from advanced analysis techniques that include CFD. Under flooding conditions, the bridges are not only subjected to increased drag and lift forces, but may also be at failure risk due to the accelerated erosion of the river bed at bridge support structures. Formation of scour depends on the flow field and turbulence conditions, sediment bed composition, sediment transport, sediment entrainment rates, and sediment settling rates. Analysis of scour hole development under bridge decks and around the bridge piers is important for both the safe design of new bridges and evaluation of flood failure risk for existing bridges.

Ramamurthy et al., [1], analyzed an open channel flow by using the Volume of Fluid (VOF) model. A two-dimensional two equation standard $k-\varepsilon$ turbulence model was used for the simulation using a PISO (Pressure Implicit with splitting of Operators) algorithm. Their simulation predictions for the pressure and velocity distributions showed close agreement with the experimental results. Koshizuka et al., [2], simulated the free surface of a collapsing liquid column for an incompressible viscous flow using VOF technique and found good agreement between simulation and experimental results. Huang et al., [3] used the Reynolds Averaged Navier-Stokes (RANS) equation to model the turbulence phenomenon for open channel flow problems.

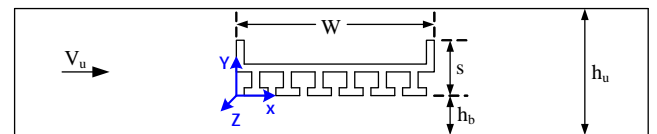
Heather D. Smith, [4], presented a modeling technique for contraction scour generating flow around a horizontal stationary cylinder by using the two-phase volume of fluid (VOF) methodology using FLOW-3D, a commercial CFD code. A comprehensive review of pipeline or completely submerged horizontal cylinder scour at a sea bed was also given in this study. Guo, [5], discussed the Shields-Rouse equation for the calculation of critical shear stress based on the experimental results and its application to sediment transport. This equation provides a correlation to determine the critical shear stress for the initiation of sediment motion as a function of dimensionless sediment diameter. Singh, [6], developed an integrated two-dimensional sediment transport model to simulate sediment transport in water. Both the suspended load and bed load have been taken into account in his study. Camenen et al., [7] proposed a new empirical correlation between the roughness height and some of the important hydrodynamic and sediment parameters for plane beds under steady flow conditions. Zhao and Fernando, [8], performed CFD simulation using the FLUENT commercial CFD code for the evolution of scour around pipelines using an Eulerian-Eulerian partially decoupled two-phase model for fluid and particulate phases. They investigated the effect of different sediment transport modes such as bed-load, suspended-load, and laminated load on the development of scour.

The objective of this study is to develop a computer simulation model to analyze the turbulent open channel flow and resulting forces on laboratory scale bridge decks and formation of scour holes under different pressure flow scour

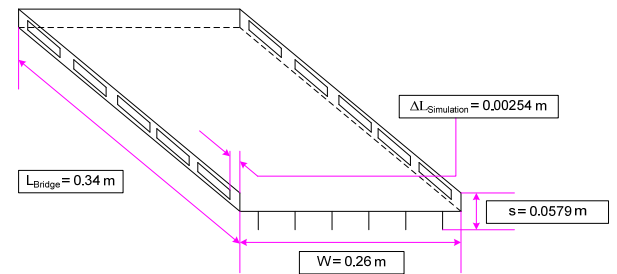
flooding conditions using STAR-CD software. The work is first focused on the CFD analysis of an open channel turbulent flow and resulting stresses on the bridge-deck and channel-bed. Further, the CFD analysis is extended to predict the depth and contour of the equilibrium scour hole beneath a flooded bridge deck under pressure flow scour conditions accounting for sediment removal only with no deposition of entrained sediment. In this effort, a computational methodology is developed and implemented in STAR-CD to predict the equilibrium of scour hole shape and size using a single phase moving boundary formulation using computation of clear water shear stress over the sediment bed contour with scouring based on excess shear above the critical shear stress.

3. DESCRIPTION OF THE PHYSICAL MODEL

A schematic of the flow channel configuration for flow over a six-girder bridge deck and the bridge dimensions are shown in Figure 1. This is a representation of the lab-scale experimental set-up used in the FHWA hydraulics laboratory, located at the Turner-Fairbank Highway Research Center (TFHRC) in McLean, VA [9, 10].



(a) Characteristic dimensions for the channel and the bridge



(b) Basic dimensions of the bridge deck

Figure 1: Schematic and dimensions of the channel bridge deck

The experiments were conducted in a rectangular flume with clear sides and a bottom made of stainless steel. The test section was located near the middle of the flume length where the model deck was immersed to model flooding conditions. For the scour experiments, sand with a median diameter (d_{50}) of 1 mm was used. A specially designed force balance set-up was used by TFHRC to measure the lift and drag forces around the bridge without scour under flat bed conditions. Simulations were based on the experimental set-up information provided by TFHRC. A two-dimensional model was used in this study assuming the effects of flume side walls may be neglected. The

holes in the bridge deck railing were also neglected as a first approximation to allow for two-dimensional analysis.

Computational Parameters

The following dimensionless parameters were used for the presentation of results.

Froude Number (Fr):

Froude number is defined as the ratio of flow velocity to the velocity of the waves at a particular location. In other words, it is the ratio of inertial forces to the gravity forces given as:

$$Fr = \frac{V_u}{\sqrt{gL_c}} \quad (1)$$

where L_c = the channel depth.

Inundation Ratio (h^*):

The inundation ratio, h^* is a measure of flooded water level over the bridge deck and is defined as

$$h^* = \frac{h_u - h_b}{s} \quad (2)$$

A value of $h^* = 1$ represents a just immersed condition of the bridge deck, whereas $h^* > 1$ represents the condition of a fully-submerged bridge deck.

Coefficient of Drag (C_D):

$$C_D = \frac{F_D}{0.5\rho V_u^2 A_F} \quad (3)$$

Coefficient of Lift (C_L):

$$C_L = \frac{F_L}{0.5\rho V_u^2 A_p} \quad (4)$$

4. COMPUTATIONAL MODEL FOR FLOW FIELD AND RESULTING FORCES

Determination of water flow forces on flooded bridge decks and the prediction of scour formation beneath the bridge deck require computation of local stresses over the bridge deck and at the flume bed. Options available for analyzing turbulent open channel flows are either a time-averaged approach using Reynolds Averaged Navier-Stokes (RANS) equations with turbulence closure models or an approach using Large Eddy Simulations (LES) that requires turbulence model closure at the small eddy scale, generally requiring transient three dimensional analysis, highly refined grids, and large computation times. In this study, the simulation is restricted to RANS turbulence models. A number of turbulence models including high-Re $k - \varepsilon$, low-Re $k - \varepsilon$, $k - \omega$ SST high-Re, and $k - \omega$ standard high-Re were applied in this study and compared against experimental data.

Simulation Based on Single-Phase Model

Simulation of open channel flows over a bridge deck, having geometry and operating conditions corresponding to the laboratory tests performed at TFHRC, were carried out using STAR-CD Version 4.04. Open channel flow was simulated by using a single-phase model without considering any interaction at the water-air interface. The top surface of the water channel was assumed to be flat with a free slip boundary condition.

Boundary Conditions

Boundary conditions are shown in Figure 2.

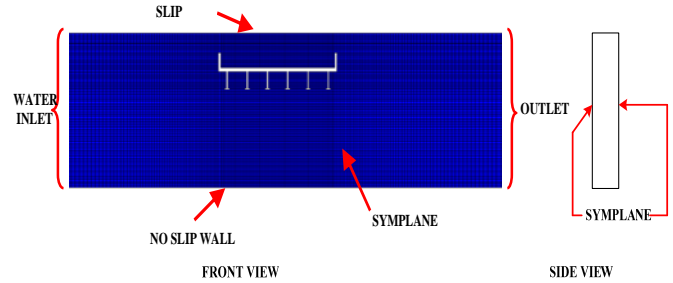


Figure 2. Boundary conditions for single-phase model

Inlet: Velocity and Turbulence conditions

A fully developed flow velocity profile was applied at the inlet. The profile was determined by computing the flow in a channel with no bridge deck blockage and extending its length until the velocity profile was no longer changing. The average turbulent kinetic energy (k) and dissipation rate (ε) for these flow conditions are $0.00125 \text{ m}^2/\text{s}^2$ and $0.000175 \text{ m}^2/\text{s}^3$ respectively.

Computational Algorithm

Steady state flow solutions were computed using the MARS differencing scheme and the SIMPLE algorithm with Algebraic Multigrid (AMG) solver.

Mesh Refinement Study

A non-uniform computational mesh, shown in Figure 3, is used in this study. Finer mesh size distributions are used around the bridge surfaces and at the bottom surface.

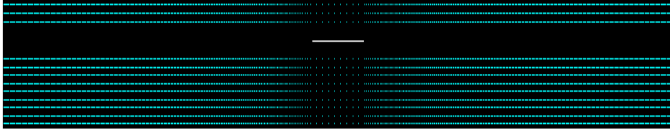
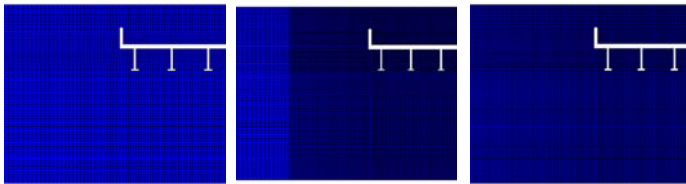


Figure 3: Mesh structure for single-phase model

A number of numerical tests were run to check sensitivity of the solution to the mesh size distribution and assigned tolerance limit for convergence. The two dimensional geometry allowed a very fine basic mesh to be used without excessive use of computer cluster resources. Two more highly refined meshes were tested to verify that the basic mesh was sufficiently fine. Sections of the three mesh size distributions near the bridge deck are shown in Figure 4. Differences in the flow field solutions for these three meshes were negligible including values of the computed drag and lift coefficients. Therefore, the basic mesh was considered to be fine for parametric computations of the effects of varying bridge depth.



(a) Basic mesh (b) Refined near bridge (c) Fully refined

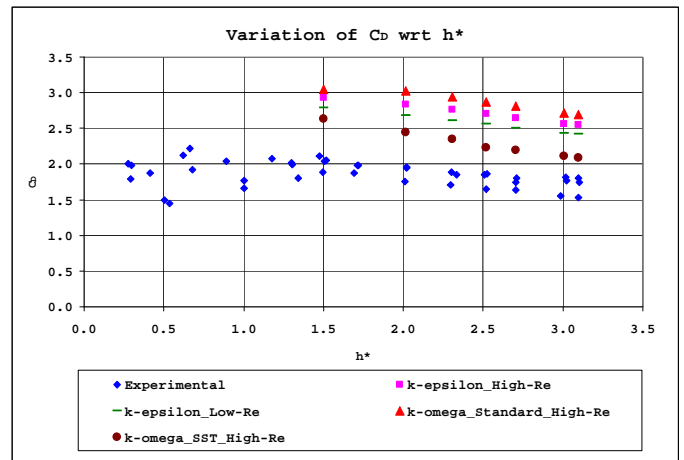
Figure 4 Tested mesh refinements

Comparison and Validation of Computational Models

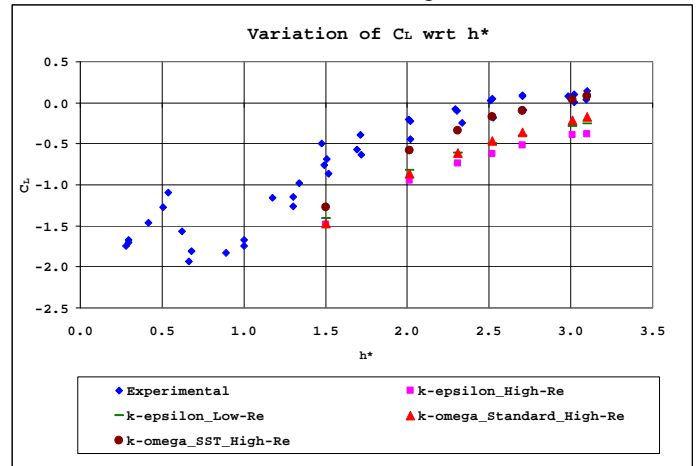
Simulation of open channel flow over a six-girder bridge deck, having a geometry and operating conditions corresponding to the laboratory tests performed at TFHRC [9.10], was carried out using the STAR-CD CFD software. The objective was to validate the simulation model with data obtained from experiments conducted at TFHRC. The experiments included lab-scale tests of open channel flow over inundated bridge decks force balance measurements of lift and drag forces for different inundation ratios and flow conditions. The data provided by TFHRC included five sets of experiments, each set containing 12 or 13 experiments for different flooding heights corresponding to a Froude number range of 0.12 to 0.40 and upstream velocity range of 0.3507 m/s to 0.3513 m/s. The experimental data was then averaged over multiple trials to obtain values of drag and lift coefficients as a function of non-dimensional bridge height, h^* . Results for Froude number, $Fr = 0.22$ are shown in Figure 5.

Results using the single-phase model and the previously defined boundary conditions, in general, follow the variation trends of both drag and lift coefficients with the variation of h^* obtained from experimental data, as shown in Figure 5. However, predictions obtained using the model overpredicted the drag coefficient and under-predicted the lift coefficient. For

example, the deviation for the high Re k -epsilon model ranged from about 50% at $h^* = 1.5$ to about 20% at $h^* = 3.0$. A variety of turbulence closure models were tested to determine if any would give results that fall within the range of data scatter, and although a k -omega model came significantly closer, none of the tested turbulence models gave results that fell within the range of experimental data scatter. A visit to the experimental facility with observation of the running flume revealed that the flow at the bridge deck test section was likely far from being fully developed. This difference in the inlet conditions may be responsible for a large portion of the difference between drag and lift coefficients obtained from experiment and CFD. Modeling approaches to more closely approximate flume inlet conditions are being pursued.



(a) Coefficient of drag



(b) Coefficient of lift

Figure 5: Drag and lift coefficients for single-phase model

5. SIMULATION MODEL FOR SCOUR ANALYSIS

Simulating the scour formation process in the sediment bed under the bridge deck due to accelerated turbulent flow is very complex due to the presence of multiple physical processes at the fluid-solid particle interface at the sediment bed. This

includes the increased turbulence and wake formations, sediment particle suspension and transport, fluid particle interactions, particle-particle interactions, and coupling between the scour profile and the two-phase turbulent flow field.

A number of modeling options are possible and have been investigated by different researchers as discussed in the introduction section. These include: (1) the empirical model of Guo [9] based on one dimensional flow theory, employing a semi-analytical solution for flow hydrodynamics and empirical correlation for the critical shear stress at the fluid-sediment interface; (2) modeling scouring as two-phase flow having water over a heavy sediment laden fluid using the volume of fluid (VOF) transient method as used by Smith, [4], and (3) an Eulerian two-phase model with partially uncoupled governing equations for fluid and solid sediment transport used by Zhao and Fernando, [8]. While two-phase modeling options, such as, VOF and Eulerian two-phase models, have the potential for greater accuracy as more detailed physics models are included, they are computationally more complex and impose significant challenges for modeling interfacial interactions and constitutive properties of the scoured materials.

The computational methodology used in this study is based on using single-phase computational fluid dynamics analysis of the flow fields around the bridge deck assuming increased turbulence under the bridge and development of increased shear stress over the bed contour can be used to obtain a conservative estimate of an equilibrium scour hole profile without considering the sediment transport. The onset of sediment motion and the formation of the scour hole are assumed to occur when the induced local bed shear stress at the sediment bed surface exceeds a critical shear stress value given by an empirical correlation. The computational methodology involves computation of local bed shear stress using CFD followed by expanding the water computational domain at the sediment bed surface, where local shearing stresses are higher than the critical shearing stress (corresponding to the threshold of the packed bed resistance to scouring), to form the scour hole profile. Such an approach significantly simplifies the mathematical and computational difficulties associated with the two-phase fluid-solid coupled transport model. One of the main challenges of this approach is to identify critical shearing stress correlations that account of all the complexity of packed bed resistance to scouring.

Since the turbulent flow field, turbulence, and the induced bed shear stress are influenced by the choice of turbulence model, a comprehensive evaluation of turbulence models is needed to determine if RANS models are adequate for the conservative prediction of scour. Initial development of scour formation methodology and implementation in STAR-CD code is carried out using a high Reynolds number *k-epsilon* model along with a standard wall-function treatment that accounts for wall roughness.

Empirical Correlation for Critical Shear Stress at Channel Bed:

In general, the critical shearing stress is not constant, but a local function of flow, material properties, and geometric slope of the packed bed interface in relation to the velocity direction just above the bed. Gravity increases the critical shear stress for flow up a sloped bed and decreases the critical shear stress for flow down a sloped bed. Since such a correlation depends on a number of key parameters including the fluid density, sediment particle's density and size, and does not account for all of the relevant detailed physics, it has to be determined by experiments. A comprehensive review of various approaches to determine the critical shear stress at the sediment bed of an open channel flow, is given by Singh, [6]. The following is a list of empirical correlations for critical shear stress available in the literature.

A. Shields-Rouse Formula:

One of the most widely used critical shear stress correlations for sediment transport is given by Guo [5], based on Shields-Rouse equation and fitting of the experimental data:

$$\frac{\tau_c}{(\rho_s - \rho)gd_{50}} = \frac{0.23}{d_*} + 0.054 \left[1 - \exp\left(-\frac{d_*^{0.85}}{23}\right) \right] \quad (5a)$$

Where

$$d_* = \left[\frac{(\rho_s / \rho - 1)g}{\nu^2} \right]^{1/3} d_{50} = \text{Dimensionless diameter} \quad (5b)$$

B. Shields Formula based on Shield's Coefficient:

Shield's parameter (θ) is defined as

$$\theta = \frac{\tau_c}{(\gamma_s - \gamma)d_{50}}, \quad (6)$$

and the critical shear stress can be calculated if the critical Shields parameter is known from the above equation.

C. USWES Formula:

The United States Waterways Experiment Station, [8], proposed an equation for the critical shear stress which is valid for a particle size of 0.205 mm to 4.077 mm having a uniformity coefficient (M) in the range of 0.28 to 0.643. The expression is as below.

$$\tau_c = 0.00595 \left((S - 1) \frac{d}{M} \right)^{1/2} \quad (7)$$

D. Chang's Formula:

Chang proposed a formula for a sediment size range of 0.134 mm to 8.09 mm and uniformity coefficient range of 0.23 to 1.0. The specific gravity of the sediment needs to be in the range 2.05 to 3.89 in order to use this equation, which is presented below.

$$\tau_c = 0.0045 \left((S-1) \frac{d}{M} \right)^{1/2} \text{ if } \left((S-1) \frac{d}{M} \right) > 2.0 \quad (8a)$$

$$\tau_c = 0.00635 \left((S-1) \frac{d}{M} \right) \text{ if } \left((S-1) \frac{d}{M} \right) < 2.0 \quad (8b)$$

E. Sakai Formula:

The formula, proposed by Sakai, [8], for critical shear stress calculation is:

$$\tau_c = \frac{100(S-1)d^{6/5}}{3} \left(\frac{2+M}{1+2M} \right) \quad (9)$$

F. Chien and Wan Formula:

Chien and Wan, [8], have developed a relationship between Shield's parameter and a non-dimensional diameter d_* to find out the critical shear stress, as shown below.

$$\theta = \begin{cases} 0.126d_*^{-0.44}, & d_* < 1.5 \\ 0.131d_*^{-0.55}, & 1.5 \leq d_* \leq 10 \\ 0.0685d_*^{-0.27}, & 10 \leq d_* \leq 20 \\ 0.0173d_*^{0.19}, & 20 \leq d_* \leq 40 \\ 0.0115d_*^{0.3}, & 40 \leq d_* \leq 150 \\ 0.052, & d_* \geq 150 \end{cases} \quad (10)$$

Where d_* is given by Equation 5b and θ is the Shield's parameter.

Based on all the above formulas, the variation of critical shear stress with the mean particle diameter has been computed and presented in figure 6.

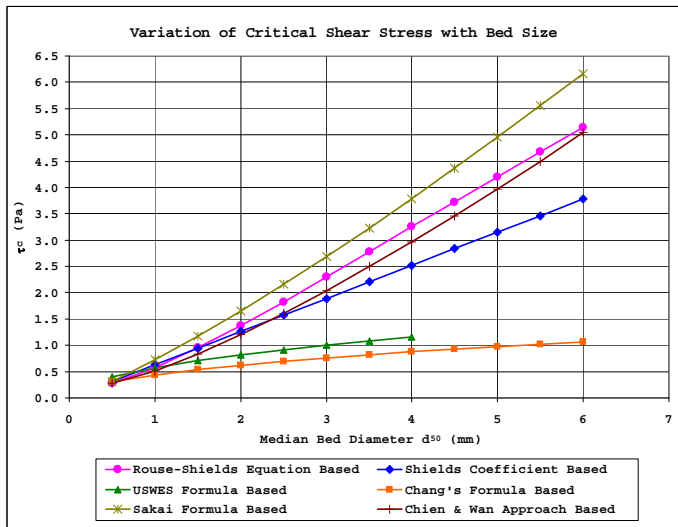


Figure 6: Variation of critical shear stress with the mean sediment size.

Results show that at small sediment sizes, for example at a median sediment diameter of 1.0 mm, the critical shear stress from all formulae are close. However, at larger diameters, Chang's formula and USWES formula (correlated in the range of 0.205 mm to 4.077 mm) show a large variation of the order of 100% as diameter is increased from 1 mm to 2 mm. For the other correlations, a large variation of critical shear stress is also apparent. At the mean sediment diameter of 1 mm used in this study, the critical shear stress varies from 0.43 Pa to 0.72 Pa depending upon the correlation used to calculate it.

The critical shear stress also depends on the suspended load and the bed load. This effect is accounted for in a correlation given by Van Rijn, [11]:

$$\frac{q_b}{d^{1.5} \sqrt{\frac{(\rho_s - \rho_w)g}{\rho_w}}} = 0.053 \frac{\left[\frac{\tau - \tau_c}{\tau_c} \right]^{2.1}}{d^{0.3} \left[\frac{(\rho_s - \rho_w)g}{\rho_w v^2} \right]^{0.1}} \quad (11)$$

where q_b = Bed load transport rate in m^2/s ,

This study is limited to scour in a saltation mode with minimal bed load, and the critical shear stress is calculated from the Shields-Rouse correlation given by Equation 5.

Effective Bed Roughness

Computational solutions of the flow field and the local shear stress, and subsequently the computed scour hole shape at the sediment bed surface, are strongly influenced by the selection of the effective surface roughness value for the sediment bed surface. The bed roughness value can vary considerably depending on the type of bed form and sediment transport regime. Sediment size and density as well as the sediment bed geometry influence the sediment transport rate and the resulting stresses at the bed surface. The total shear stress values are typically measured in an experimental test set-up, and empirical relations are developed for the effective bed roughness. These correlations express roughness values as a function of median grain diameter and Shield's parameter (θ), which represents the sediment transport rate in terms of bed friction velocity or critical shear stress. The functional form also depends on the type of bed forms, which is influenced by the order of magnitude of the sediment transport rate. The sediment transport regimes are classified into three different types: (1) a saltation regime with plane bed form at low sediment transport rates ($\theta < 0.5$) (2) bed sheet flow without suspension, and (3) bed sheet flow with suspension. The last two regimes occur with higher sediment transport rates having $\theta > 0.5$.

A list of such functional relations and detailed discussion on the development of the relations are given by Camenen et al. [7]. A new functional correlation based on their experimental study is also proposed that includes dimensionless settling velocity and Froude number in addition to the Shield's parameter. An evaluation of these experimental correlations for sand considering $d_{50} = 1$ mm and Shields parameter, $\theta = 0.039$

showed considerable scatter in the effective roughness values varying by a factor of 1 to 6 greater than the sediment median size. In order to determine an appropriate effective roughness value for use in the simulation model, a number of trial computations were carried out for flow over the bridge deck and the flat-bottom surface with bed roughness values ranging from 1 mm to 6 mm. Results for shear stress distribution at the bed surface are shown in Figure 7.

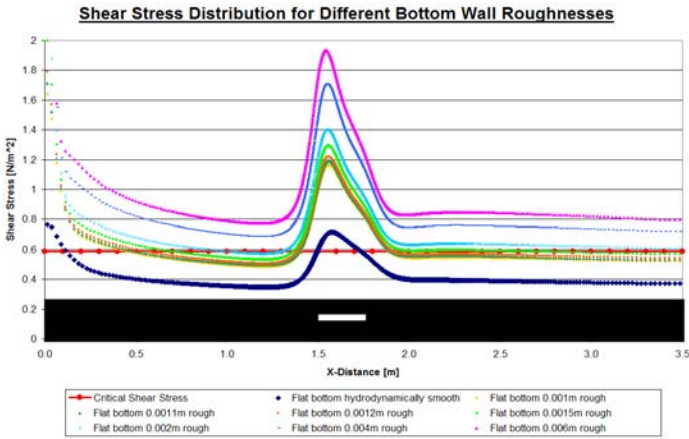


Figure 7: Flat bed shear stress distribution with different bed roughness values

Results show that predicted local shear stress values over the bed surface is a strong function of the roughness and that they increase with increased roughness. The shear stress distribution for an equilibrium scour hole surface should reach a level that is lower than the critical shear stress distribution over the entire surface. This result indicates that the effective bed roughness will have a strong influence on the scour hole depth. Numerical experiments can be performed with different effective bed roughness values while using the iterative simulation methodology to determine an effective roughness that yields a best match to experimental scour hole depth. This value can then be used for additional analysis and compared against experiment to test its range of applicability.

Simulation Based on Experimental Scour Profile

In order to determine an effective roughness value, flow simulation is carried out for the flow channel with the experimental scour profile obtained at TFHRC [9] with different bed roughness values. These simulations compute the flow field and the local shear stress, using a known scour profile. In order to use a smooth bed profile very close to the experimental scour profile, Guo's [10] proposed exponential curve-fit expressions of the scour hole profile with depth y_s are adopted. The functional relation is given as follows.

$$\text{For } x \leq 0, \quad \frac{y}{y_s} = -\exp\left(-\left|\frac{x}{W}\right|^{2.5}\right) \quad (12a)$$

and

$$\text{for } x \geq 0, \quad \frac{y}{y_s} = -1.055 \exp\left[-\frac{1}{2}\left(\frac{x}{W}\right)^{1.8}\right] + 0.055 \quad (12b)$$

where $x = 0$ is defined as the position of maximum scour. Guo [10] included a constant term of 0.055 in equation (12b) in order to capture the sediment deposition phenomenon downstream of the trailing edge of the obstacle. Guo's formula agrees reasonably well with experimental results, having a relative error in the range 3 to 16%.

Figure 8 shows the local stress distribution using different bed roughness values from 1.2 mm to 3 mm for the case with $h_u = 25$ cm, $h_b = 11.5$ cm, $s = 4$ cm.

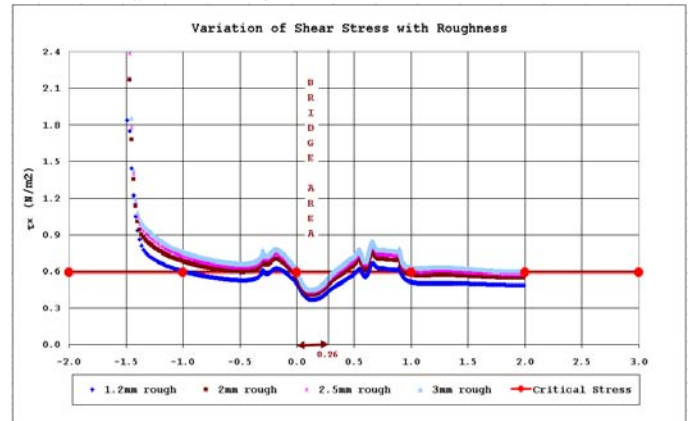


Figure 8: Distribution of shear stress along the bed surface using different roughness values

Results in Figure 8 show that local shear stress distribution at the scour-hole surface fell below the constant critical shear stress value of 0.58 N/m^2 for a relative roughness of 2 mm, which is about twice the median sediment diameter considered, after the inlet flow development region, under the deck, and about three deck widths downstream of the deck. Shear stress is high at the inlet due to an assumed uniform velocity at the inlet. The goal here is to identify a roughness value that produces a shear stress distribution downstream of the inlet development region that is closest to the critical value.

Implementation of Clear Water Equilibrium Scour Prediction Methodology in STAR-CD

The single-phase simulation model is run iteratively with re-meshing between each run to determine the scour hole shape by incrementally moving the bed surface at locations where the local shear stress values exceeded the critical value. Flow calculation is repeated with the newly formed geometry after re-meshing. This iteration process of flow calculation and creation of the new scour bottom is repeated until it approaches sub-critical shear stress over most of the bed surface giving an equilibrium scour hole profile.

The scour hole is created by removing all cells at the bottom surface where the local shear stress value τ , is higher than the critical shear stress value τ_c . The cell removal scheme

is based on the magnitude of deviation of computed shear stress from the critical shear stress. Bed material can be removed using very fine increments where bed shear stress exceeds the critical value. Some initial simulation results showed that this approach is computationally stable, but requires a large number of iterations and excessive computer time. In an alternative approach, the scour profile depth at any location is increased based on the magnitude of the local shear stress deviation from the critical value using the following equation:

$$\Delta y = \Delta y_s \left(\frac{\tau - \tau_c}{\tau_{\max} - \tau_c} \right) \quad (13)$$

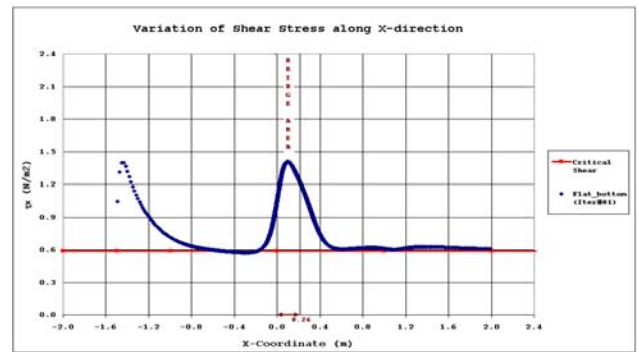
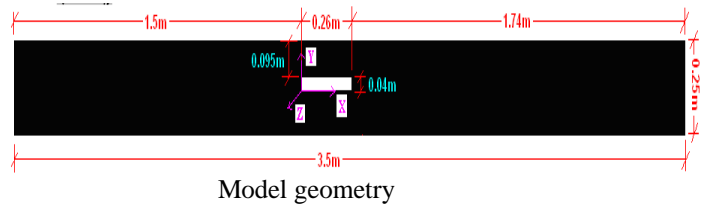
According to this formula, the higher the shear stress value with respect to the critical, the deeper the scour hole in the next iteration. The basic approach involves increasing the maximum scour depth by $y_s = y_s + \Delta y_s$ at the location with maximum shear stress. For the rest of the bed surface, the y-locations are also moved by an incremental amount Δy , which is proportional to local shear stress values as estimated based on the equation (13). The value of Δy_s can be assigned in the beginning of the iteration process as a relatively small value and may be kept constant for all iterations. Alternatively, it can be assigned as a relatively large value in the beginning and progressively reduced at every iteration steps as the solution approaches equilibrium condition. In order to demonstrate the methodology in this preliminary test study, the selection of Δy_s is manually adjusted based on the evaluation of shear stress values and the location of maximum shear stress value after each iteration.

In the implementation of this scour simulation methodology in STAR-CD, the iterative simulation process is partially automated, using a STAR-CD command set for re-meshing and a bash script for auto-execution of STAR-CD code. Manual steps include redefining the bed contour in a spread sheet. A full automation process is being implemented in order to eliminate the need for any human intervention [12].

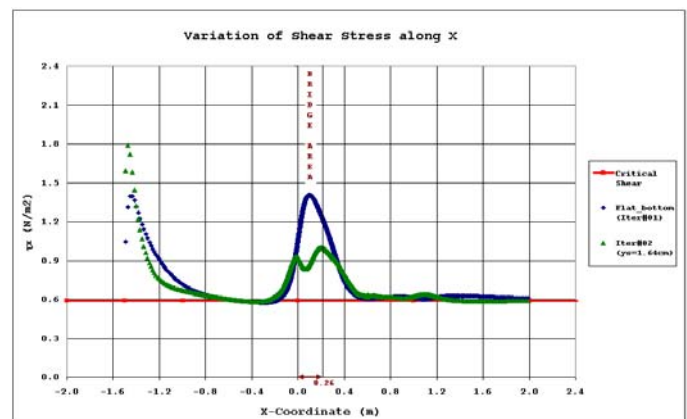
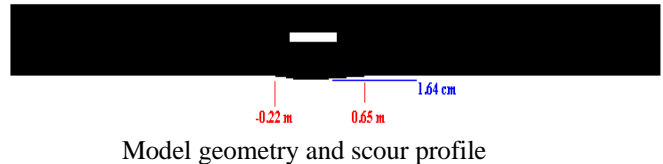
6. RESULTS AND DISCUSSION

The geometry and simulation conditions used in the computational domain for initial scour evolution study are as shown in Figure 2. To simplify the problem for initial tests, the six-girder bridge geometry was replaced with a rectangular block with the same aspect ratio as of the six-girder bridge. The operating conditions and other geometric parameters correspond to the following values: upstream velocity = 0.41 m/s, channel size: $h_u = 25$ cm and $h_b = 11.5$ cm. The critical shear stress value is 0.58 Pa based on 1 mm sand diameter and assumed to be constant over the flat and scour hole surface. This is reasonable assumption because experimental scour hole slopes are much smaller than the angle of repose for the sand. The effective bed roughness is taken to be 2 mm for a median sediment diameter of $d_{50} = 1$ mm. The simulation results for eight iteration steps

with bed re-meshing are shown in Figure 9. Both the scour shape profile and the shear stress distribution at the scoured bed are shown.



(a) Initial Shear stress distribution for flat bottom surface

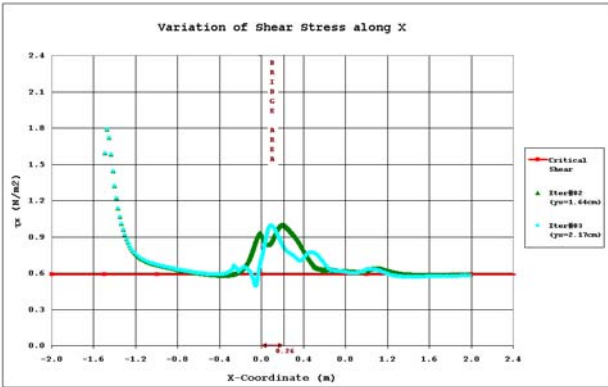


Shear stress
(b) Iteration # 02



-0.26 m 1.0 m 2.17 cm

Scour Profile



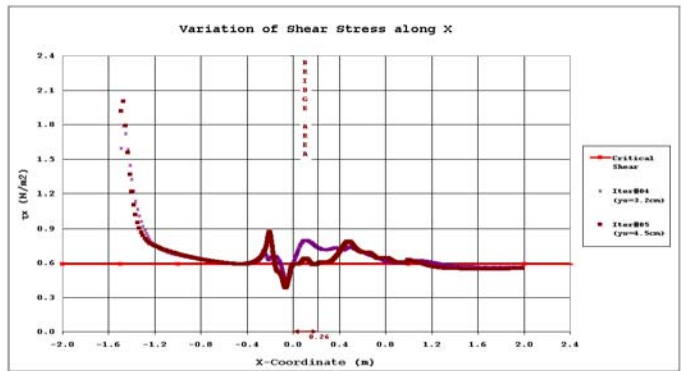
Bed shear stress distribution

(c) Iteration # 03



-0.36 m 1.0 m 4.5 cm

Scour profile



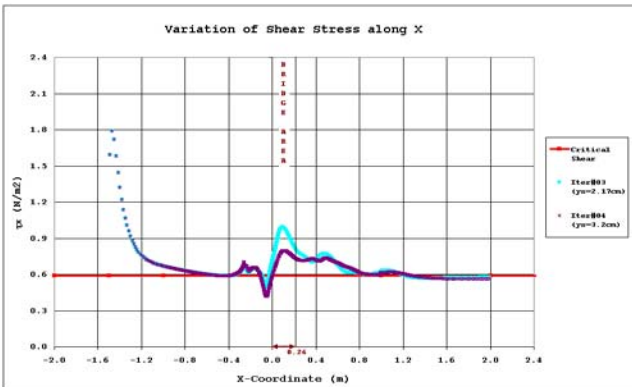
Shear stress distribution

(e) Iteration # 05



-0.26 m 1.0 m 3.2 cm

Scour Profile



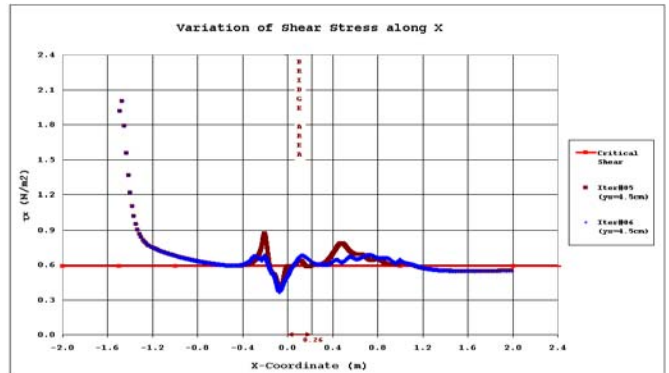
Bed shear stress distribution

(d) Iteration # 04



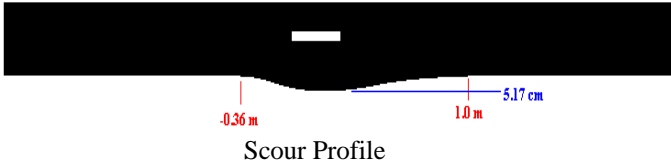
-0.36 m 1.0 m 4.5 cm

Scour Profile

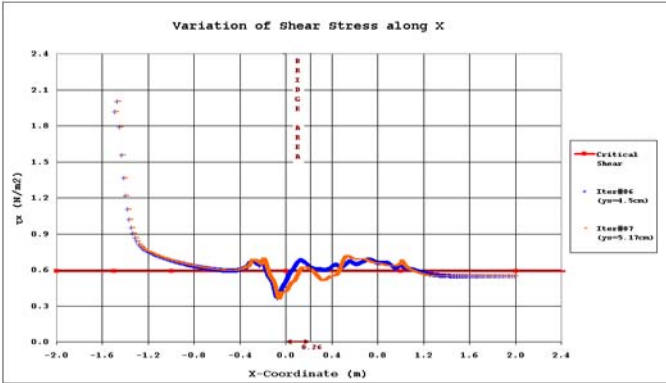


Bed shear stress distribution

(f) Iteration # 06

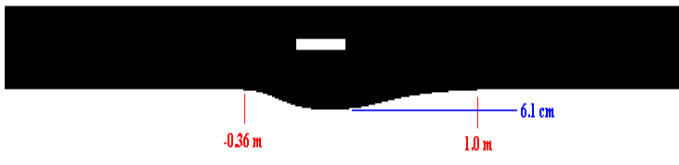


Scour Profile

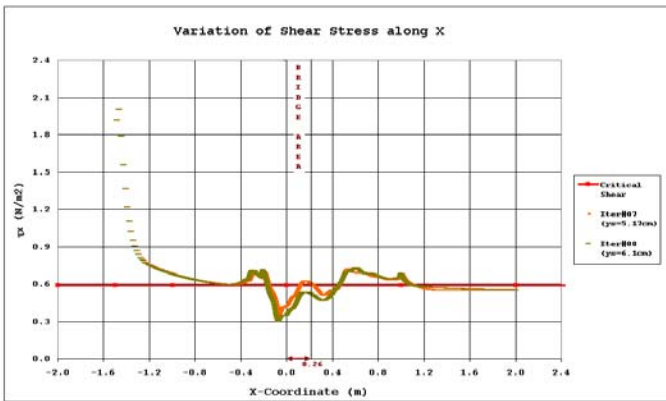


Bed shear stress distribution

(g) Iteration #07



Scour Profile



Bed shear stress distribution

(h) Iteration #08

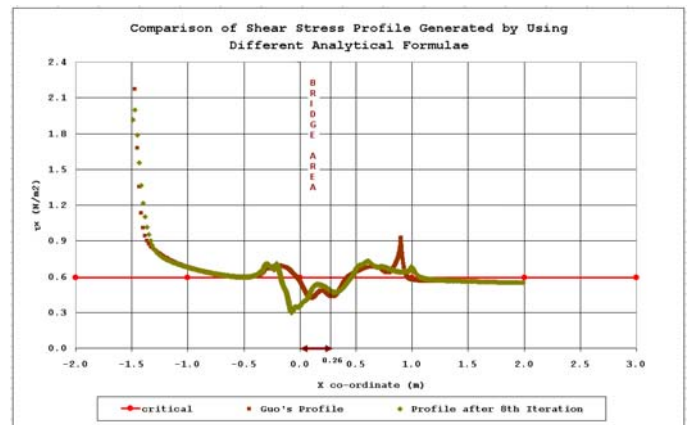
Figure 9 Variation of bed scour profile and bed shear stress distribution for different bed re-meshing iterations.

Results show iterative estimation of the scour hole and continuous decrease in the bed surface shear stress with iterations. The final scour hole profile and the local shear stress distribution as obtained in the iteration step # 8 show that the shear stress distribution fell below the critical shear for most of the regions of the bed under the bridge deck. However, it shows overcritical shear stress values at the leading and trailing end of the scour profile. This may be caused by the insufficient smoothing of the scour profile as it is merged with the flat bed

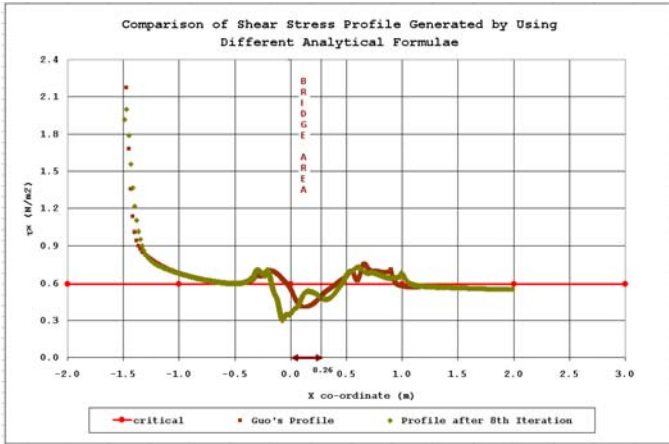
surface and the associated mesh distribution. In addition, the critical shear stress will not be constant over the scour hole. The magnitude of these effects has not been determined in this study. The objective of this study was focused primarily on demonstrating the iterative methodology for determining an equilibrium scour profile. In order to decrease the computational time a relatively coarse bed adjustment step size was used and adjusted manually while removing the cells during evolving scour profile at each iteration step. Under these conditions completing a set of runs took more than a week. The accuracy and smoothness of the scour hole profile may be improved significantly by using a much finer step size, Δy_s . Additionally, the iteration computing procedure and the final results for scour profile may be improved with the use of a varying critical shear stress profile that takes into account of the angle of the bed slope.

Comparison of Simulation Results with Experiment

Figure 10 shows the comparison of shear stress distribution obtained for the simulated scour hole shape with that obtained for the experimental scour shape given by equation (12). Results show similar shear stress profiles except at the leading edge of the scour profile where simulation estimates lower shear stress on the down slope of the scour hole. Additional discrepancy also occurs at the downstream side of the bridge where a spike can be seen for the analytical shear stress profile with the sediment deposition term left out because the simulations did not model sediment transport and deposition downstream of the scour hole. Figure 10b shows a closer match of shear stress profiles at the downstream side between the simulated results and the experimental curve-fit profile when the deposition term in equation (12b) is included. Not accounting for sediment transport and deposition is considered a reasonable first approach to the problem because it is conservative in the sense that it will not under predict the scour depth.



(a) Sediment deposition term of '0.055' not included in curve-fit scour profile



(b) Sediment deposition term of '0.055' included in curve-fit scour profile

Figure 10. Comparison of shear stress distribution along scoured bed given by the computational model and experimental curve-fit scour profile

Effect of Scouring on Force Coefficients

Formation of a scour hole has a significant effect on the resulting lift and drag forces on a flooded bridge deck. Figure 11 shows the variation of resulting drag and lift forces in terms of coefficient of drag and lift over the bridge deck for the scour hole shape obtained at each iterative step. Results show that the drag force decreases with the increase of scour hole depth, which results in an increase in water flow area in the approach to the bridge deck and consequently reduces the velocity of water impinging on the deck and near deck surfaces and the resulting stresses. On the other hand, there is a stronger negative lift force as the scour-hole increases with iterations. Both drag and lift forces approach equilibrium values with increase in iteration steps as the scour-hole profile also reaches equilibrium shape.

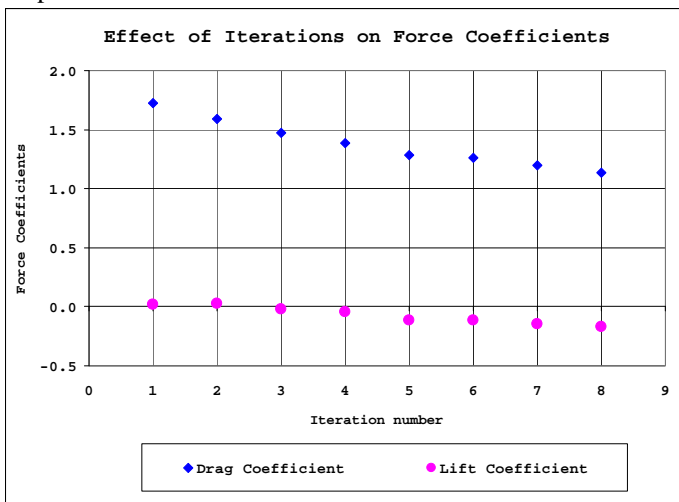


Figure 11: Variation of force coefficients with iteration

7. CONCLUSIONS

Computational fluid dynamics simulation for turbulent open channel flow over inundated bridge decks was performed to determine the resulting forces around a flooded model bridge deck and the equilibrium scour hole at the channel bed under the deck. The fluid dynamics model used a single-phase model and did not account for sediment transport and deposition in the downstream. An iterative computational methodology was used to predict the equilibrium scour hole by increasing the bed depth between simulation runs based on excess shear above critical shear stress for onset of particle motion. A comparison of the simulated results for scour profile and the corresponding shear stress distribution with experimental results showed reasonable agreement for maximum scour depth and the distribution of shear stress at the mid-section of the scour hole profile. The deviation of shear stress profile over the scour bed is quite significant at the leading edge of the scour profile. Refinement of the iterative procedure for adjusting scour hole depth may improve the smoothness of the shear profiles obtained during the iterated runs and allow a complete automation of the process with a clearly defined convergence criteria.

8. REFERENCES

[1] Ramamurthy, A.S., Qu, Junying, Vo, Diep. (2005), "Volume of fluid model for open channel flow problem", *Canadian Journal of Civil Engineering*, Vol. 32, No.5, pp 996-1001, 2005.

[2] Koshizuka, S., Tamako, H., Oka, Y., (1995), "A particle method for incompressible viscous flow with fluid fragmentation", *Computational Fluids Dynamics Journal*, Vol.4, pp 29-46, 1995.

[3] Huang, J., Lai, Y.G., Patel, V.C., (2001), "Verification and validation of 3-D numerical model for open channel flows", *Numerical heat Transfer part B*, Vol. 40, pp 431-439, 2001.

[4] Smith, Heather D., (2004), "Modeling the flow and scour around an immovable cylinder", M.S. Thesis, Ohio State University.

[5] Guo, J., (2002) "Hunter Rouse and Shields Diagram", *Advances in Hydraulic and Water Engineering*, Vol. 2, pp.1096-1098, 2002.

[6] Singh, Vikas, (2005), *Two dimensional sediment transport model using parallel computers*, M.S. Thesis, Banaras Hindu University, India.

[7] Camenen, Benoit, Bayram, Atilla, and Larson, Magnus, (2006), Equivalent Roughness Height for Plane Bed

under Steady Flow, *Journal of Hydraulic Engineering*, vol. 132, No. 11, November 1, 2006.

[8] Zhao, Zhihe and Fernedo, H. J. S., (2007), “Numerical Simulation of Scour around Pipelines Using an Euler-Euler Coupled Two-phase Model”, *Journal of Fluid Mechanics*, Vol. 7, pp 121-142, 2007.

[9] Guo, J., Kerenyi, K., Pagan-Ortiz, J. E. and Flora, K., (2009), “Bridge Pressure Flow Scour In Clear Water Threshold Condition”, *Transaction of Tianin University*, Vol. 15, No. 2, 2009,

[10] Turner-Fairbanks Highway Research Center (TFHRC): <http://www.fhwa.dot.gov/engineering/hydraulics/research/lab.cfm>. Accessed June, 2009.

[11] Van Rijn, L. C., (1984) “Sediment transport I: Bed load transport”, *Journal of Hydraulic Engineering*, Vol. 110, No. 10, 1431-1456, 1984.

[12] Biswas, D., (2009), Computational Fluid Dynamics Simulation and Analysis of Open Channel Flow and Scouring under Different Bridge Flooding Conditions with the help of an Automated Iterative Procedure, M. S. Thesis, Department of Mechanical Engineering, Northern Illinois University, 2009.

[13] Adhikary, B. D., (2008), Flow and Pressure Scour Analysis of an Open Channel Flow Having an Inundated Bridge Deck Under Various Flooding Conditions, M. S. Thesis, Department of Mechanical Engineering, Northern Illinois University, 2008.

9. ACKNOWLEDGEMENTS

The authors would like to acknowledge support by Dean Promod Vohra, College of Engineering and Engineering Technology, Northern Illinois University, Dr. David P. Weber and Dr. Tanju Sofu of Argonne National Laboratory for their contribution, as well as the computational support by Argonne’s Transportation Research and Analysis Computing Center, and lastly financial support by United States Department of Transportation.

The submitted manuscript has been created by UChicago Argonne, LLC, Operator of Argonne National Laboratory (“Argonne”). Argonne, a U.S. Department of Energy Office of Science laboratory, is operated under Contract No. DE-AC02-06CH11357. The U.S. Government retains for itself, and others acting on its behalf, a paid-up nonexclusive, irrevocable worldwide license in said article to reproduce, prepare derivative works, distribute copies to the public, and perform publicly and display publicly, by or on behalf of the Government.

COPYRIGHT INFORMATION

Proceedings of the
ASME 2009 International Mechanical Engineering Congress & Exposition
November 13-19, 2009 • Lake Buena Vista, Florida, USA

Copyright © 2009 by ASME
All rights reserved

ISBN 978-0-7918-3863-1
Order No. I830DV

ASME shall not be responsible for statements or opinions advanced in papers or discussion at meetings of ASME or its Divisions or Sections, or printed in its publications (Statement from ASME By-Laws, 7.1.3).

This material is distributed by ASME "AS IS" and with no warranties of any kind; ASME disclaims any warranty of accuracy, completeness, or timeliness. ASME will not be held liable to the user or any other person for any damages arising out of or related to the use of, results obtained from the use of, or any inability to use, this DVD. Users assume all risks.

This is a single-user product. Permission to download, print, and photocopy a single individual copy of any of the works contained on this DVD for personal use in research and/or educational pursuit is granted by ASME.

Requests for permission to use this ASME material elsewhere, to make electronic copies, or to use on LAN/WAN hardware should be addressed to permissions@asme.org. Please note that a licensing fee for the wider application and distribution of this material on LAN/WAN hardware will be assessed.

Requests for reprints of any of the ASME material on this DVD should be directed to reprints@asme.org.

Adobe Acrobat Reader is a registered trademark of Adobe Systems Incorporated. Adobe Acrobat Reader is freely available for distribution, and may be obtained at the Adobe website at <http://www.adobe.com/acrobat/main.html>.

The search technology used on this DVD is a registered trademark of JObjects and has been licensed for use with this DVD.